Aggregation structure of Alzheimer amyloid-β(1–40) peptide with sodium dodecyl sulfate as revealed by small-angle X-ray and neutron scattering

Jihh-Min Lin,[ab] Tsang-Lang Lin,*[a] U-Ser Jeng,*[c] Zyun-Hua Huang[a] and Yu-Shan Huang[c]

Received 24th April 2009, Accepted 24th June 2009
First published as an Advance Article on the web 3rd August 2009
DOI: 10.1039/b908203d

Using small-angle X-ray scattering (SAXS) and small-angle neutron scattering (SANS) with contrast variation, we have studied the complex aggregation of Alzheimer amyloid-β(1–40) (Aβ) peptides with sodium dodecyl sulfate (SDS). With the addition of 0.115 mM Aβ peptide into an aqueous solution containing 6 mM SDS, time-dependent SAXS indicates the formation of a globular SDS–Aβ complex with a core–shell structure. The emergence of the complex aggregates, however, lags significantly behind the fast transition of the secondary structure of Aβ peptides from random coil to α-helical structure observed by circular dichroism (CD). With scattering contrast varied by SDS and deuterated SDS, SANS results reveal the coexistence of Aβ aggregates and the SDS–Aβ complex, which together form clusters of a mass fractal structure. Based on the changes of the zero-angle scattering intensity with the contrast variation, a molecular association ratio, ~30 : 1, of SDS to Aβ is extracted for the globular complex micelle. With a concentration (20 mM) above the critical micelle concentration (CMC) of SDS, time-dependent SAXS and CD reveal a better synchronization between the formation of the SDS–Aβ complex and the changes in Aβ secondary structure. Using an ellipsoid model with a core–shell structure in the SAXS data analysis, we have extracted detailed structural information of the prolate, core-shelled SDS–Aβ complex, having size and shape resembling pure SDS micelles. The significantly larger electron density of the shell of the complex, as compared to that of pure SDS micelles, suggests that the hydrophilic parts of Aβ peptides can situate well with the sulfate headgroups of SDS in the shell region. Delicate differences in the micellar structure and the formation pathway of the two types of SDS–Aβ complexes, respectively formed in aqueous solutions containing SDS concentrations below and above its CMC, are discussed in terms of the dissimilar association efficiencies of Aβ peptides with SDS monomers and SDS micelles. The morphology, association ratio, and clustering behavior of the SDS–Aβ complex obtained in this study may have implications in interpreting the related spectroscopy and SDS–PAGE results of the protein.

1. Introduction

Containing 39–43 amino acid residues, Amyloid-β (Aβ) peptide is a fragment derived from proteolytic cleavage of the large amyloid precursor protein (APP) of Alzheimer's disease.[1] Extensively studied with various tools,[2–9] Aβ peptides have been shown to convert to β-sheet structure in aqueous solutions, and then pleated β-sheets were able to stack and grow into spiral fibrils with a helix pitch of 24 β-strands.[3] As the senile plagues containing Aβ fibrils were originally observed from the cellular membranes of patients with Alzheimer's disease, considerable studies focused on the growth behavior of Aβ peptides in the presence of membrane or surfactant interfaces,[10–20] in search of implications that may lead to efficient ways of reducing or preventing Aβ fibrils. One of the many approaches focuses on the interactions of the water-soluble Aβ peptides with sodium dodecyl sulfate (SDS) micelles of polar surfaces. Elucidated by circular dichroism (CD), nuclear magnetic resonance (NMR), fluorescence, and electron microscopy, SDS micelles were shown to be able to efficiently suppress the formation of the toxic β-sheet structure of Aβ peptides;[6,7,21] it was also found that below the critical micelle concentration (CMC), SDS monomers might interact with Aβ peptides differently.[6,7,21]

Despite that the suppression effect of SDS on Aβ fibril formation has been clearly demonstrated in several studies,[6,7,21] the discussions on the related mechanism were essentially based on the changes of the secondary structure of Aβ peptides observed by CD. The CD spectra, however, were insensitive to developments of complex aggregates of Aβ peptides with SDS. Very recently, the SDS–Aβ complex micelle structure was studied using NMR and a paramagnetic probe:[22] based on the responses of the Aβ residues to the controlled environment, residues were grouped and positioned either outside, inside, or near the surface of the SDS micelle. To shed more light on the molecular mechanism of the formation of SDS–Aβ complex aggregates and their role in the suppression of Aβ aggregation, we focus on the aggregation structure of the complex micelle in this study, including size, shape, association ratio, and formation

[a]*Department of Engineering and System Science, National Tsing Hua University, 101, Sec. 2, Kuang Fu Road, Hsinchu 300, Taiwan; Fax: +886-3-5728445; Tel: +886-3-5742671*
[b]*Research School of Chemistry, The Australian National University, Canberra ACT 0200, Australia*
[c]*National Synchrotron Radiation Research Center, 101 Hsin-Ann Road, Hsinchu Science Park, Hsinchu 30076, Taiwan; Fax: +886-3-578-3813; Tel: +886-3-578-0281, ext 7108*

process; the direct structural information should also bear implications in interpreting the related spectroscopy and SDS–PAGE results of the protein.[19]

In the structural characterization of Aβ peptides or their aggregates in solutions, small-angle neutron scattering (SANS)[2,10] and small-angle X-ray scattering (SAXS)[9] have demonstrated their sensitivity in detecting the protein morphology and aggregation structure. In resolving structures of complex aggregates, the combination of SANS and SAXS is particularly advantageous as demonstrated in our previous studies.[24–26] Adopting the same scattering based methodology, we have resolved two types of SDS–Aβ complexes, respectively, formed in solutions with SDS concentrations below (but near) and above the CMC of SDS.[27] With SDS in the peptide–surfactant complex replaced by deuterated SDS (d-SDS), we have furthermore extracted the partial aggregation numbers of SDS and Aβ peptides for the complex aggregates. The delicate differences in the micellar structure and the formation pathway of the two types of SDS–Aβ aggregates are discussed in terms of the characteristically different associations of Aβ peptides with SDS monomers (of disperse sulfate headgroups) and SDS micelles (of organized charge shells).

2. Materials and methods

Sample preparation and measurements

Alzheimer amyloid-β peptide, with 1–40 amino acid residues and a molecular weight $M_w = 4329.8$ g mol^{-1}, was received from Sigma and Biopeptide Co. After being dissolved in hexafluoroisopropanol (HFIP) for 12 hours, the peptide was retrieved by lyophilization in the form of monomers, and subsequently redissolved (0.115 mM Aβ or 0.5 mg ml^{-1}) in 10 mM Na_3PO_4 buffer solutions, containing 6 and 20 mM sodium dodecyl sulfate (SDS), respectively. For comparison, a solution with 0.115 mM Aβ peptide was also prepared. For all sample solutions, there were no extra salts added. The critical micelle concentration (CMC) of SDS in pure water is 8 mM,[28] which is about the same with 1 mM HCl (pH = 3) added.[29] Unless specified, the CMC of SDS referred to in this study is mainly for pure SDS solutions rather than for mixtures with Aβ peptides.

SANS measurements were conducted on the 30 m small angle neutron scattering spectrometer at the National Institute of Standards and Technology (NIST), Gaithersburg, USA. Regular SDS and deuterated SDS (d-SDS) were used in preparing sample solutions with D_2O for the varying of the scattering contrast of the peptide–surfactant complexes with respect to D_2O. The sample solutions were sealed in quartz cells at 25 °C, and measured with 5 Å neutrons at two sample-to-detector distances of 2.5 m and 15 m, for a wide Q-range. The scattering wavevector $Q = 4\pi\lambda^{-1}\sin\theta$ is defined by the scattering angle 2θ and wavelength λ of neutrons (or X-rays in SAXS). The SANS data collected were corrected for transmission, background, and pixel sensitivity of the 2-D detector, and circularly averaged into one-dimensional (1-D) intensity distribution function $I(Q)$. The data were further scaled to the absolute scale (in units of cm^{-1}) defined by the scattering cross-section per unit sample volume. We emphasize the importance of using the absolute intensity scale in obtaining partial aggregation numbers of complex aggregates.[25,26]

The sample solutions for SAXS measurements were prepared using the same procedures as that for SANS, except that 1 mM HCl was added to each sample solution to speed up Aβ peptide aggregation for *in situ* SAXS measurements within a reasonable time interval of ~48 h synchrotron beamtime. SAXS measurements were conducted at the BL17B3 SWAXS end-station of the National Synchrotron Radiation Research Center (NSRRC), Taiwan. Details of the instrument were reported previously.[30] In this study, a 0.5 mm diameter beam with 1.24 Å (10 keV) X-rays and a sample-to-detector distance of 2.7 m were used. The sample solutions were sealed in sample cells by two thin Kapton films (8 μm each) for an X-ray path length of 2.2 mm. SAXS data collected with a 2-D (20 cm × 20 cm) gas detector at 25 °C were processed with a similar procedure as that used for the SANS data. The scattering intensity was scaled to the absolute scale *via* the scattering of a standard polyethylene sample.

Data analysis

The SANS or SAXS intensity distribution for colloidal solutions is often described by $I(Q) = I_0P(Q)S(Q)$, where $I_0(Q = 0)$ is the zero angle (forward) scattering, $P(Q)$ the normalized form factor, *i.e.* $P(Q = 0) = 1$, and $S(Q)$ the structure factor.[23] For spherical particles, $P(Q) = [3j_1(Qr)/Qr]^2$, with the first-order spherical Bessel function $j_1(Qr)$. For homogeneous rod-like particles of radius R and length L, the spatial-orientation averaged form factor is expressed as:

$$P(Q) = \int_0^1 \left[\frac{2J_1(v)}{v}\frac{\sin(w)}{w}\right]^2 \mathrm{d}\mu' \quad (1)$$

with $v = QR(1 - \mu'^2)^{1/2}$, $w = (1/2)QL\mu'$, and J_1 is the first order Bessel function.[23] The often-used Schultz distribution[31,32] can be incorporated into eqn (1) for polydispersity in rod length. For core–shell spheres or ellipsoids,

$$P(Q) = \int_0^1 \left[\frac{W_1 - W_2\frac{V_1}{V_2}}{W_1 + W_2}3j_1(u_1) + \frac{W_1 + W_2\frac{V_1}{V_2}}{W_1 + W_2}3j_1(u_2)\right]\mathrm{d}\mu'' \quad (2)$$

where $u_1 = Q[a^2\mu''^2 + b^2(1 - \mu''^2)]^{1/2}$, $u^2 = Q[(a + T)^2\mu''^2 + (b + T)^2(1 - \mu''^2)]^{1/2}$, with the semi-major and semi-minor axes a and b for the core, and shell thickness T; W_1 and W_2 are the respective scattering contrasts of the core and shell with respect to the solvent, whereas V_1 and V_2 are the corresponding volumes.[33]

For systems with a fractal dimension D and a correlation length ξ, the structure factor can be expressed as:

$$S(Q) = 1 + \frac{1}{(Qr)^D}\frac{D\Gamma(D-1)}{\left(1 + (Q\xi)^{-2}\right)^{(D-1)/2}}\sin\left[(D-1)\tan^{-1}(Q\xi)\right] \quad (3)$$

with radius r for the primary particles that constitute the fractal structure.[34]

The forward scattering $I_0(Q = 0)$ of the complex aggregates containing partial aggregation numbers N_p for Aβ peptides and N_s for SDS, can be described by

$$I_0 = n_p[N_p(b_p - \rho_w V_p) + N_s(b_s - \rho_w V_s)]^2 \quad (4)$$

with b_p, b_s and V_p, V_s denoting, respectively, the scattering lengths and dry volumes of the Aβ peptide and SDS;[25,26,33,36] whereas n_p is the number density of the complex aggregate and ρ_w the scattering-length-density of solvent. Replacing SDS by d-SDS, we can drastically change the b_s value in eqn (4), thus, the I_0 value. Based on eqn (4) with the calculated b_p, b_s, V_p, V_s and ρ_w values (from the related chemical formulae) and two measured I_0 values of $I_{0,sds}$ and $I_{0,d\text{-}sds}$, we can deduce a relation for the molecular association ratio of SDS to Aβ:

$$\mu = N_s/N_p = A(\chi - 1)/(\chi B_d - B) \quad (5)$$

where $A = b_p - \rho_w V_p$, $B_d = b_{s,d\text{-}sds} - \rho_w V_s$, $B = b_{s,sds} - \rho_w V_s$, and the squared root of the zero-angle scattering intensity ratio $\chi = \pm(I_{o,sds}/I_{o,d\text{-}sds})^{1/2}$. The partial aggregation numbers of Aβ and SDS can be furthermore derived as $N_p = (I_{0,sds}/n_p)^{1/2}/(A + \mu B)$ and $N_s = \mu N_p$.

3. Results and discussion

Growth of pure Aβ peptide aggregates

Shown in Fig. 1 are time-dependent SAXS data of the pure Aβ peptide solution measured, respectively, at 12, 22, and 36 h after sample preparation. The nearly two-orders-of-magnitude increase in intensity over the measuring time indicates a drastic growth of the peptide aggregates. The later two sets of SAXS data reveal characteristics of a rod-like structure (linear region in the inset of Fig. 1), and can be fitted with a common rod diameter $2R$ of 86 ± 6 Å using the Kratky–Porod approximation.[26] The result implies that rod-like Aβ peptide aggregates mainly grow in length towards fibril structure, while maintaining a constant rod cross-section. These structural features are consistent with that observed in the previous SANS measurements by Yong *et al.*[2] and Thiyagarajan *et al.*,[10] as well as our own atomic force microscope (AFM) images displaying prototype fibrils with a uniform rod diameter of ~85 Å. Taking into account the polydispersity effect in rod length (as described by the Schultz distribution), we can fit (Fig. 1) the three sets of SAXS data using a rod-like form factor.[26] The structural parameters extracted from the non-linear least-square fitting algorithm indicate that the prototype fibrils of Aβ peptides grow continuously from a rod length of 100 Å at 12 h, 180 Å at 22 h, to 440 Å at 36 h, while maintaining a constant rod diameter of 92 Å and a relatively large polydispersity of *ca.* 100% in length.

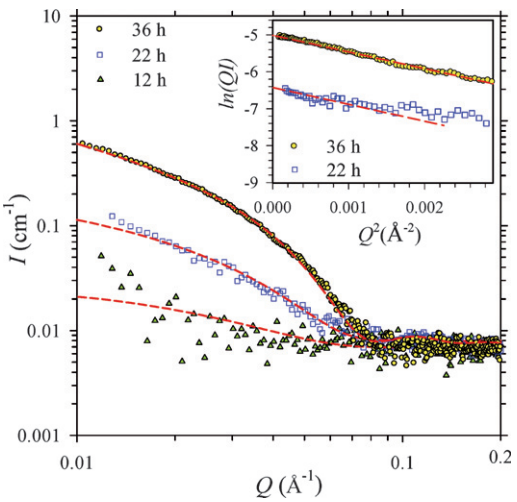

Fig. 1 SAXS data of the aqueous solutions of 0.115 mM (0.5 mg ml^{-1}) Aβ peptide with 1 mM HCl measured, respectively, at 12 h, 22 h, and 36 h after sample preparation. The data are fitted (dash curves) using a rod form factor with polydispersity in rod length. The inset shows the two sets of the data measured at 22 h and 36 h, respectively, fitted with the Kratky–Porod approximation (dashed lines).

Formation of SDS–Aβ aggregates below the CMC of SDS

Shown in Fig. 2 are the SAXS data measured at t = 10 h, 30 h, and 48 h, after mixing 0.115 mM Aβ peptide with 6 mM SDS. The scattering intensity in the low Q-region (<0.04 Å^{-1}) increases with time and gradually develops into the power-law scattering behavior of $I(Q) \propto Q^{-4}$ (inset of Fig. 2), implying the formation and growth of large Aβ aggregates. The change in SAXS profile essentially terminates around $t \approx 30$ h, indicating a shorter growth period than that observed in pure Aβ aggregation (*cf.* Fig. 1). The shorter growth period associates closely with the appearance of the scattering hump in the Q-region of ~0.08–0.2 Å^{-1} in the SAXS profile, which signifies the formation of a SDS–Aβ complex with a core–shell structure similar to SDS micelles.[19,27,28] The peak position of the hump at Q = 0.132 Å^{-1}, however, is significantly smaller than that (Q = 0.177 Å^{-1}) of pure SDS micelles,[27,28] indicating larger SDS–Aβ complexes than SDS micelles. Using the sphere form factor with a core–shell structure (eqn (2)), we can adequately fit (dashed curve in Fig. 2) the SAXS data measured at t = 30 h (in the Q-region of 0.08–0.20 Å^{-1}), with a core radius of 25.2 Å and a shell thickness

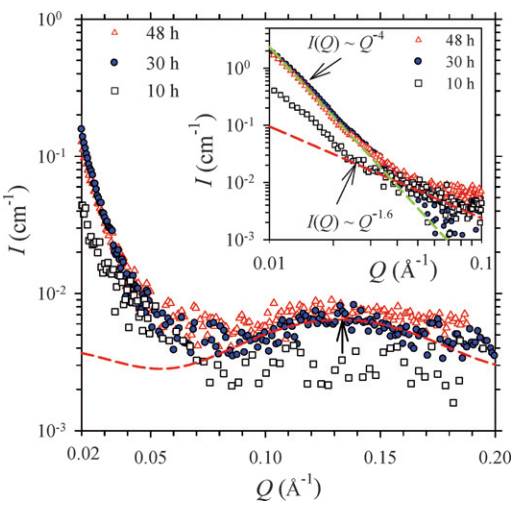

Fig. 2 SAXS data measured at t = 10 h, 30 h, and 48 h, after mixing 0.115 mM Aβ peptide with 6 mM SDS and 1 mM HCl. The data collected at t = 30 h are fitted (dashed curve) using a sphere form factor with a core–shell structure, in the Q region ~0.08 to 0.20 Å^{-1}. The arrow indicates the peak position (0.132 Å^{-1}) of the core–shell hump. In the inset, indicated by the arrows and the fitted dotted lines are the two regional power-law scatterings: $I(Q) \approx Q^{-4}$ contributed by large Aβ aggregates in the low-Q region and $I(Q) \approx Q^{-1.6}$ by clusters of the SDS–Aβ complex in the intermediate Q-region.

of 4.2 Å. For comparison, prolate SDS micelles have a smaller ellipsoidal core size, with semi-major axis $a = 21.8$ Å, semi-minor axis $b = 16.5$ Å, and a shell thickness of 4.3 Å (as detailed below). We notice that there is also a power-law scattering feature of $I(Q) \approx Q^{-1.6}$ in the SAXS profiles in the intermediate Q-region (inset of Fig. 2), which can be attributed to a mass-fractal-like clustering of SDS–Aβ complex micelles with pure Aβ aggregates, as more clearly distinguished by SANS with contrast variation below.

SANS with contrast variation for partial aggregation numbers of SDS–Aβ complex

To extract more structural details of the SDS–Aβ complex revealed in the SAXS results, we have furthermore measured SANS for the two contrast-varied sample solutions of 0.115 mM Aβ peptide mixed, respectively, with 6 mM deuterated and non-deuterated SDS. As shown in Fig. 3, in the low-Q region ($\lesssim 0.005$ Å^{-1}) the two SANS profiles overlap well and exhibit the same power-law scattering of $I(Q) \propto Q^{-4}$ as that observed in the SAXS; the insensitive scattering to the SDS contrast variation is attributed to large Aβ aggregates with little or no SDS content. In contrast, the scattering intensity in the larger Q-region ($\gtrsim 0.01$ Å^{-1}), including the power-law scattering feature $I(Q) \propto Q^{-1.6}$ (corresponding to a mass fractal dimension of 1.6),[34] drops dramatically by nearly 6 fold when SDS in the system is replaced by d-SDS, implying that the scattering in this Q-region highly associates with SDS-related aggregates and their clustering *via* a mass fractal structure. We emphasize that in D_2O solution, the scattering contrast of d-SDS, of a scattering length density (SLD) $\rho = 6.8 \times 10^{-6}$ Å^{-2}, with respect to D_2O ($\rho = 6.4 \times 10^{-6}$ Å^{-2}) is much smaller than that of SDS ($\rho = 0.4 \times 10^{-6}$ Å^{-2}) and Aβ peptide ($\rho = 0.3 \times 10^{-6}$ Å^{-2}) with respect to D_2O.[25,26] Therefore, d-SDS in D_2O is nearly invisible to neutrons. On the other hand, without forming micelles 6 mM SDS monomers contribute little structural features in the SANS profile, as illustrated in Fig. 3.

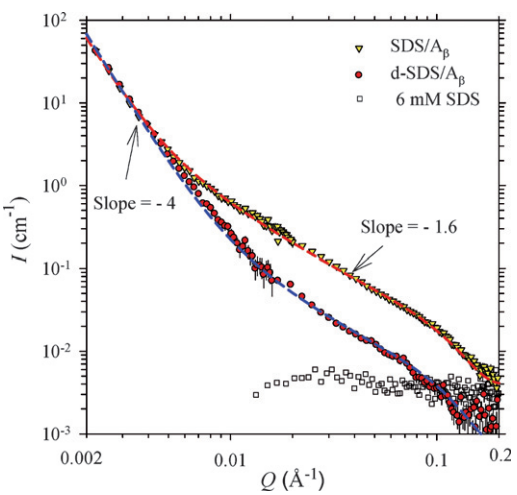

Fig. 3 SANS data for the aqueous solutions of 0.115 mM (0.5 mg ml^{-1}) Aβ peptide mixed with 6 mM SDS and 6 mM d-SDS, respectively. The two sets of data are fitted (dashed curves) with the same sphere form factor and the same fractal structure factor of a mass fractal dimension $D = 1.6$ (indicated by the arrow) in the intermediate Q-region. The low-Q data are fitted with the power-law scattering $I(Q) \propto Q^{-4}$. For comparison, SANS data for the solution of 6 mM SDS are also shown.

There is, however, no discernable core–shell hump in the SANS profiles (*cf.* Fig. 3), likely due to the low scattering contrast between the D_2O solvent and the hydrated shell. In fact, neutrons are mainly scattered by the aliphatic core of the complex micelle in D_2O; whereas X-rays are more sensitive to the core–shell structure, due to the higher electron density of the shell than that of the core and solvent. Therefore, in fitting the SANS data, we adopt a simple sphere form factor for the SDS–Aβ complex and a fractal structure factor for the power-law scattering characteristics of $I(Q) \propto Q^{-1.6}$ (observed in the intermediate Q -region ~0.01–0.07 Å^{-1}).[34] As a result, we can fit well the two sets of contrast SANS data in Fig. 3, with the common structure parameters of radius $r = 21$ Å, mass fractal dimension $D = 1.6$, and correlation length $\xi = 430$ Å (corresponding to a cluster size $\sim 2\xi = 860$ Å), for the complex aggregates.[34] In the fitting algorithm, we have also included the Q^{-4} contribution from large Aβ aggregates in the low-Q region ($Q \lesssim 0.006$ Å^{-1}). The obtained complex size from SANS is nevertheless slightly smaller than that ($r = 25.2$ Å) extracted from the SAXS result. Using eqn (5), we have furthermore deduced the SDS–Aβ association ratio $\mu = 30 \pm 2$ for the peptide–surfactant complex using the two I_0 values extrapolated from the two sets of contrast variation SANS data in Fig. 3. The molecular association ratio of 30 corresponds to a weight ratio of 1.9, which is reasonably close to the general weight ratio of 1.4 (SDS to protein) established for a wide variety of proteins that bind to SDS.[38] Adopting the CMC of Aβ aggregation $c^* = 0.035$ mM reported by Yong *et al.*,[2] we have further deduced the partial aggregation numbers $N_p = 2 \pm 0.4$ and $N_s = 60 \pm 12$, using the relation $N_p = I_0(Q = 0)/[(c - c^*)(\Delta\rho_p V_p + \mu\Delta\rho_s V_s)^2]$, with the scattering contrasts of the peptide-solvent $\Delta\rho_p$ and the SDS-solvent $\Delta\rho_s$, the dry volumes of V_p (5470 Å^3) and V_s (400 Å^3), and the Aβ peptide concentration c.[25,26]

The derived SDS aggregation number, 60 ± 12, of the complex is sufficiently higher than the minimum number ~42 for forming a pure SDS micelle.[28] With the high association ratio $\mu = 30$, Aβ peptides can be well-surrounded by the outnumbered surfactants in the complex micelles and segregated from the rest of the peptides, thus, aggregation is suppressed.

In general, the SANS results are consistent and complementary to the previous SAXS result, especially in revealing the fractal structure of a low mass fractal dimension of 1.6; the structure is attributed to a clustering of the core–shell complexes *via* the mediation of residual Aβ aggregates. In contrast, there is no such fractal structure observed when Aβ aggregates are completely suppressed by sufficient SDS micelles (see the results described below). Likely, with insufficient SDS monomers, incomplete (or partial) complex micelles containing Aβ peptides can also detour and act as compartments (nuclei) to dense Aβ peptides for limited Aβ aggregation; these Aβ aggregates in turn loosely interconnect neighboring matured complex micelles for clusters of a mass fractal structure.[34] Interestingly, similar loosely connected protein–surfactant clusters with features of mass fractal structure were also reported in several studies,[19,34,35,37–39] especially those with low surfactant concentrations.[6,21]

SDS–Aβ complex micelles formed above the CMC of SDS

Shown in Fig. 4 are the SAXS data measured at $t = 10$, 22, and 48 h after mixing 0.115 mM Aβ peptide with 20 mM SDS.

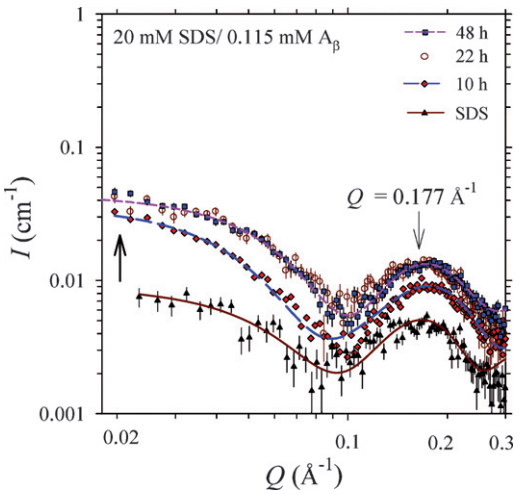

Fig. 4 SAXS data measured at 10, 22, and 48 h, after mixing 0.115 mM (0.5 mg ml^{-1}) Aβ peptide with 20 mM SDS and 1 mM HCl. Also shown are the SAXS data for the solution with 20 mM SDS and 1 mM HCl. The data are fitted (solid and dashed curves) using a core–shell ellipsoid form factor. The two arrows indicate the significant growth of I_0 in the low Q-region and the stable core–shell hump of the SDS–Aβ complex micelles in the high Q-region.

At $t = 10$ h, a significant increase in the I_0 value and enhanced core–shell hump features around $Q = 0.177$ Å^{-1}, as compared to that for pure 20 mM SDS micelles, can already be observed. The result reveals faster kinetics of complex formation of Aβ peptides with pre-existing SDS micelles (namely, the fast adsorption of Aβ peptides to the SDS micelles), as compared to the case of 6 mM SDS monomers (*cf.* Fig. 2) or the slow formation of pure Aβ fibrils (*cf.* Fig. 1). Between $t = 22$ to 48 h, neither the I_0 value nor the core–shell hump change significantly; the small and stabilized I_0 value indicates the absence of large Aβ aggregates, whereas the absence of fractal-like scattering features in the SAXS profiles implies that the SDS–Aβ complex micelles are well dispersed and do not form clusters.

Adopting a core–shell ellipsoid form factor[33] for the SDS-micelle based complex (*cf.* eqn (2)), we can adequately fit (dashed curves in Fig. 4) the time dependent SAXS profiles for the structural evolution of the SDS–Aβ complex and pure SDS micelles. The fitted parameters, summarized in Table 1, indicate that the adsorption of the peptides to the pre-existing SDS micelles in the earlier time ($t \lesssim 10$ h) causes an elongation of the prolate SDS micelles in the semi-major axis, from $a = 23.8$ Å to 47.7 Å and a minor contraction in the semi-minor axis from $b = 19.5$ Å to 17.0 Å; the shell thickness of the complex, $T = 4.4$ Å, is nearly the same as that for pure SDS micelles. Between $t = 22$ and 48 h (based on the SAXS data measured at $t = 22$ h and 48 h), the complex micelles have reorganized to a more compact size ($a = 27$–30 Å, $b = 18$–19 Å, $T = 4.5$ Å) which is slightly larger than pure SDS micelles. Note that the fitted X-ray scattering-length-density of the shell of the complex micelle, $\rho \approx 13.5 \times 10^{-6}$ Å^{-2}, is substantially higher than that (12.6×10^{-6} Å^{-2}) of pure SDS micelles (mainly anionic headgroups with hydrated water molecules).[28] Since Aβ peptides have a higher X-ray scattering-length-density ($\rho = 13.5 \times 10^{-6}$ Å^{-2}) than water (9.47×10^{-6} Å^{-2}) and the aliphatic core of SDS (7.86×10^{-6} Å^{-2}),[25,26] the result implies that the adsorbed Aβ peptides can accommodate their hydrophilic parts into the shell region (of ~4–5 Å thickness) of the complex micelle with the SDS headgroups (which may expel some of the hydrated water molecules into solution), leading to the increased mean electron density of the shell observed.

Table 1 Structural parameters for the SDS–Aβ complex and SDS micelles obtained from the time-dependent SAXS data in Fig. 4, using a core–shell ellipsoid form factor with the semi-major and semi-minor axes a and b of the core, shell thickness T, and scattering-length-density of the shell ρ_{sh}

	a/Å	b/Å	T/Å	$\rho_{sh}/10^{-6}$ Å^{-2}
Pure SDS	23.8	19.5	4.8	12.6
SDS–Aβ (10 h)	47.7	17.0	4.4	13.4
SDS–Aβ (22 h)	27.1	18.6	4.5	13.5
SDS–Aβ (48 h)	29.7	17.9	4.6	13.5

CD results

Shown in Fig. 5 are the CD spectra measured for the 0.115 mM Aβ peptide in solutions with 6 mM and 24 mM SDS, respectively. These spectra exhibit the strong characteristics of α-helical structure, having a strong positive band peak at 195 nm and two negative bands centered at 208 and 222 nm, respectively;[7] the spectra were stable during the subsequently continuous monitoring over 12 days. Compared to the slower aggregation behavior revealed by time-dependent SAXS, the changes in the secondary structure of Aβ peptides from random coil to α helix upon the addition of SDS were immediately observable after mixing the peptides with either 6 or 20 mM SDS, implying fast kinetics for the secondary structural transformation of Aβ peptides *via* their association with SDS. For comparison, the CD spectrum of a freshly prepared Aβ solution shows the characteristics of random coil structure (of a strong negative band centered at 200 nm), whereas that of an aged Aβ solution of fibril aggregates demonstrates the characteristic dip at 217 nm of the β-sheet structure. These CD results are essentially consistent with

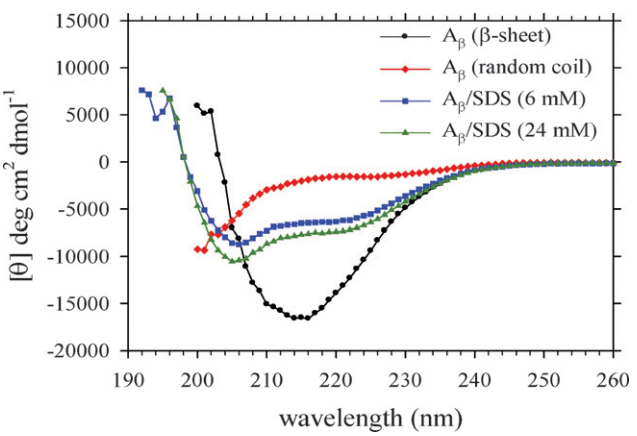

Fig. 5 Indicative of the α-helical structure are the CD spectra for the Aβ peptide solutions (0.115 mM) mixed with 6 mM and 24 mM SDS, respectively. Also shown are the CD spectra for the fresh and aged Aβ peptide solutions, respectively, revealing the corresponding random coil and β-sheet structures.

previous studies,[6,7,21] in which CD spectra for Aβ solutions with SDS concentrations above 3 mM were shown to be stable with the α-helical structure during long term observation.

Comparison of the SDS–Aβ complexes formed below and above the CMC of SDS

We have shown that with a SDS concentration of either 6 mM or 20 mM (below or above the CMC), the secondary structure of Aβ peptides can be quickly converted to the α-helical structure and stabilized. The aggregation behavior of the SDS–Aβ complexes formed in these two cases, however, differs in terms of the size, shape, and formation pathway. As revealed by the time-dependent SAXS results, with 6 mM SDS, an incubation time was needed before emergence of SDS–Aβ complex (*cf.* Fig. 2), whereas the SDS–Aβ complex could be observed earlier with the pre-existing SDS micelles at 20 mM SDS (*cf.* Fig. 4). Presumably, the pre-existing SDS micelles can effectively attract Aβ peptides *via* the well-organized anionic shells of the $SO_4^-Na^+$ headgroups, as there are seven positively charged amino acids in each Aβ peptide.[7] The adsorption of Aβ peptides to the SDS micelles and their changes in the secondary structure to the α helix should be closely associated; the transition of protein secondary structure to α-helix is often used as an indicator of protein binding to membranes.[40–42] While the Aβ peptide adsorption to SDS micelles can be fast, the subsequent relocation of the peptide in the complex micelle may require time in positioning the hydrophobic parts (mainly residues 32–40) into the core region of the SDS micelle and the hydrophilic parts (residues 1–16) into SDS anionic shell (without increasing the shell thickness by much). As suggested by the time-dependent structural parameters summarized in Table 1, the complex micelle becomes increasingly compact with time, accompanied by the gradually increased scattering-length-density ρ_{sh} of the shell. Depicted in Fig. 6 is a model for the SDS–Aβ complex based on the structural features described above. Similar positioning of the Aβ(1–40) peptide in a SDS micelle was also illustrated recently based on the results using NMR and a paramagnetic probe:[22] the two α-helices, residues 15–24 and 29–35, were placed at the surface of the micelle whereas the C-terminal helix was put inside the hydrophobic core of the micelle. Here, we provide consistent and complementary structural information for the complex micelle, including the size, shape, and growth/clustering behavior.

In forming an SDS–Aβ complex with 6 mM SDS, with no organized sulfate headgroups for a collective charge attraction, Aβ peptides are expected to interact with individual SDS monomers. The CD result indicates that 6 mM SDS monomers can still be efficient enough in transforming and stabilizing the secondary structure of the peptides to the α-helical structure. The appearance of the complex micelles, however, lags significantly behind the transformation of the secondary structure of the peptide, implying slow kinetics of the complex formation. Likely, it is the relatively bulky Aβ peptides (with a size of 5470 $Å^3$) that act as nuclei to localize sufficient SDS monomers (of a smaller volume of 400 $Å^3$) over the time for forming matured complex micelles. Such an aggregation process may involve competition between the associations of Aβ–SDS and Aβ–Aβ (for fibril aggregation); concentrations of SDS and Aβ and their respective interactions with water (*i.e.* amphiphilicity) also matter. As a result, it seems that the formation of the SDS–Aβ complex (with 6 mM SDS) was still more active than the Aβ aggregation towards fibrils, so that Aβ aggregation was largely terminated after the appearance of the complex micelles. Furthermore, competition and cooperation between the formation of the SDS–Aβ complex and residual Aβ aggregates may result in the mass-fractal clusters observed (by SANS and SAXS). Based on the association ratio μ (SDS : Aβ) $\approx$ 30 : 1 obtained from the SANS data for the solution with 0.115 mM Aβ and 6 mM SDS, we can deduce a free SDS concentration (apart from that in the complex micelles) of $\sim$ 2.6 mM. Interestingly, such an estimate is consistent with the previously CD observations[6,21] that SDS with concentrations below 3 mM could not stabilize Aβ peptides in the α-helical structure for long, and β-sheets for Aβ fibril aggregation gradually formed.

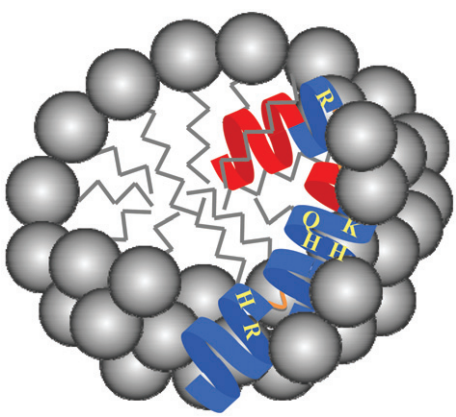

Fig. 6 Cartoon of the SDS–Aβ complex formed with pre-existing SDS micelles. The hydrophobic parts of the peptide (red blocks) hide inside the aliphatic core of the SDS micelle, whereas the hydrophilic parts (blue blocks) mainly mingle with $SO_4^-Na^+$ headgroups (solid spheres) in the anionic shell of the SDS micelle. The seven positively charged residues Arg5, His6, His13, His14, Gln16, Lys18, Arg28, are subsequently denoted R, H, H, H, Q, K, and R.

4. Conclusions

Using SAXS and SANS with contrast variation, we have extracted detailed structural information, including size, shape, partial aggregation numbers, and clustering behavior, for two types of SDS–Aβ complexes formed in aqueous solutions of Aβ peptides mixed, respectively, with 20 mM SDS (micelles) and 6 mM SDS (monomers); both types of SDS–Aβ complexes have a stable α-helical structure as suggested by the CD results. With SDS micelles pre-existing in the solution, prolate SDS–Aβ complex can efficiently form on the basis of the core–shell structure of SDS micelles, and the complex micelles remain well disperse with no observable Aβ aggregates. Whereas with 6 mM SDS monomers, globular, core–shell SDS–Aβ complexes can also form, but with slower formation kinetics that cannot fully subside Aβ aggregation. Mediated by residual Aβ aggregates, the globular SDS–Aβ complexes furthermore loosely interconnect into clusters of a low mass fractal dimension. The structural information on the SDS–Aβ complex obtained, including shape, size, fractal-like clustering behavior, and molecular association

ratio may have implications for interpreting the related spectroscopy and SDS–PAGE results of the protein.[19,43]

Acknowledgements

We thank Dr D. L. Ho for the help in the SANS measurements, and acknowledge the support of the NIST for the SANS beam time.

References

1 D. G. Lynn and S. C. Meredith, *J. Struct. Biol.*, 2000, **130**, 153.
2 W. Yong, A. Lomakin, M. D. Kirkitadze, D. B. Teplow, S.-H. Chen and G. B. Benedek, *Proc. Natl. Acad. Sci. U. S. A.*, 2002, **99**, 150.
3 T. S. Burkoth, T. L. S. Benzinger, V. Urban, D. M. Morgan, D. M. Gregory, P. Thiyagarajan, R. E. Botto, S. C. Meredith and D. G. Lynn, *J. Am. Chem. Soc.*, 2000, **122**, 7883.
4 J. D. Harper, C. M. Lieber and P. T. Lansbury, Jr., *Chem. Biol.*, 1997, **4**, 951.
5 M. G. Botelho, M. Gralle, C. L. P. Oliveira, I. Torriani and S. T. Ferreira, *J. Biol. Chem.*, 2003, **278**, 34259.
6 V. Rangachari, D. K. Reed, B. D. Moore and T. L. Rosenberry, *Biochemsitry*, 2006, **45**, 8639.
7 K. J. Marcinowski, H. Shao, E. L. Clancy and M. G. Zagorski, *J. Am. Chem. Soc.*, 1998, **120**, 11082.
8 M. Sunde, L. C. Serpell, M. Bartlam, P. E. Fraser, M. B. Pepys and C. C. F. Blake, *J. Mol. Biol.*, 1997, **273**, 729.
9 M. Gralle, M. M. Botelho, C. L. P. de Oliveira, I. Torriani and S. T. Ferreira, *Biophys. J.*, 2002, **83**, 3513.
10 P. Thiyagarajan, T. S. Burkoth, V. Urban, S. Seifert, T. L. S. Benzinger, D. M. Morgan, D. Gordon, S. C. Meredith and D. G. Lynn, *J. Appl. Crystallogr.*, 2000, **33**, 535.
11 S. J. Wood, B. Maleeff, T. Hart and R. Wetzel, *J. Mol. Biol.*, 1996, **256**, 870.
12 T. H. J. Huang, D.-S. Yang, N. P. Plaskos, S. Go, C. M. Yip, P. E. Fraser and A. Chakrabartty, *J. Mol. Biol.*, 2000, **297**, 73.
13 O. Gursky and S. Aleshkov, *Biochim. Biophys. Acta*, 2000, **1476**, 93.
14 S.-R. Ji, Y. Wu and S.-F. Sui, *Biochemistry (Moscow)*, 2002, **67**, 1283.
15 B. L. Kagan, Y. Hirakura, R. Azimov, R. Azimova and M.-C. Lin, *Peptides*, 2002, **23**, 1311.
16 N. Arispe, E. Rojas and H. B. Pollard, *Proc. Natl. Acad. Sci. U. S. A.*, 1993, **90**, 567.
17 H. Lin, R. Bhatia and R. Lal, *FASEB J.*, 2001, **15**, 2433.
18 A. Lomakin, D. S. Chung, G. B. Bendek, D. A. Kirschner and D. B. Teplow, *Proc. Natl. Acad. Sci. U. S. A.*, 1996, **93**, 1125.
19 M. Samsó, J.-R. Daban, S. Hansen and G. R. Jones, *Eur. J. Biochem.*, 1995, **232**, 818.
20 R. Sabate and J. Estelrich, *Langmuir*, 2005, **21**, 6944.
21 T. A. Pertinhez, M. Bouchard, R. A. Smith, C. M. Dobson and L. J. Smith, *FEBS Lett.*, 2002, **529**, 193.
22 J. Jarvet, J. Danielsson, P. Damberg, M. Oleszczuk and A. Graslund, *J. Biomol. NMR*, 2007, **39**, 63.
23 S.-H. Chen and T.-L. Lin, *Methods of Experimental Physics – Neutron Scattering in Condensed Matter Research*, ed. K. Sköld, and D. L. Price, Academic Press, New York, 1987, vol. 23B, (ch. 16).
24 Y.-S. Sun, U. Jeng, Y.-S. Huang, K. S. Liang, T.-L. Lin and C.-S. Tsao, *Phys. B*, 2006, **385–386**, 650.
25 U. Jeng, T.-L. Lin, Y. Hu, T. S. Chang, T. Canteenwala, L. Y. Chiang and H. Frielinghaus, *J. Phys. Chem. A*, 2002, **106**, 12209.
26 T.-L. Lin, U. Jeng, C.-S. Tsao, W.-J. Liu, T. Canteenwala and L. Y. Chiang, *J. Phys. Chem. B*, 2004, **108**, 14884.
27 S. F. Santos, D. Zanette, H. Fischer and R. Itri, *J. Colloid . Interface Sci.*, 2003, **262**, 400.
28 E. Y. Sheu and S.-H. Chen, *J. Phys. Chem.*, 1988, **92**, 4466.
29 A. Rahman and C. W. Brown, *J. Appl. Polym. Sci.*, 1983, **28**, 1331.
30 Y. H. Lai, Y. S. Sun, U. Jeng, J.-M. Lin, T.-L. Lin, H.-S. Sheu, W.-T. Chuang, Y.-S. Huang, C.-H. Hsu, M.-T. Lee, H.-Y. Lee, K. S. Liang, A. Gabriel and M. H. J. Koch, *J. Appl. Crystallogr.*, 2006, **39**, 871.
31 J.-M. Lin, T.-L. Lin, U. Jeng, Y.-J. Zhong, C.-T. Yeh and T.-Y. Chen, *J. Appl. Crystallogr.*, 2007, **40**, s540.
32 E. Y. Sheu, *Phys. Rev. A*, 1992, **45**, 2428.
33 T.-L. Lin, S.-H. Chen, N. E. Gabriel and M. F. Robers., *J. Am. Chem. Soc.*, 1986, **108**, 3499.
34 S.-H. Chen and J. Teixeira, *Phys. Rev. Lett.*, 1986, **57**, 2583.
35 C. Sun, J. Yang, X. Wu, X. Huang, F. Wang and S. Liu., *Biophys. J.*, 2005, **88**, 3518.
36 U. Jeng, T.-L. Lin, C.-S. Tsao, C.-H. Lee, L. Y. Wang, L. Y. Chiang and C. C. Han., *J. Phys. Chem. B*, 1999, **103**, 1059.
37 X. H. Guo, N. M. Zhao, S.-H. Chen and J. Teixeira, *Biopolymers.*, 1990, **29**, 335.
38 X. H. Guo and S.-H. Chen, *Phys. Rev. Lett.*, 1990, **64**, 2579.
39 K. Ibel, R. P. May, K. Kirschner, H. Szadkowski, E. Mascher and P. Lundahl, *Eur. J. Biochem.*, 1990, **190**, 311.
40 K. Matsuzaki and C. Horikiri, *Biochemistry*, 1999, **38**, 4137.
41 A. Kakio, S.-I. Nishimoto, K. Yanagisawa, Y. Kozutsumi and K. Matsuzaki, *Biochemistry*, 2002, **41**, 7385.
42 Y. Porat, S. Kolusheva, R. Jelinek and E. Gazit, *Biochemistry*, 2003, **42**, 10971.
43 K. Boland, M. Behrens, D. Choi, K. Manias and D. H. Perlmutter, *J. Biol. Chem.*, 1996, **271**, 18032–18044.